

Conductance of individual C_{60} molecules measured with controllable gold electrodes

T. Böhler, A. Edtbauer, and E. Scheer

Physics Department, University of Konstanz, D-78457 Konstanz, Germany

(Received 5 June 2007; published 27 September 2007)

We investigated the conductance of C_{60} molecules using mechanically controllable break-junction electrodes at 10 K in UHV. The molecules are evaporated *in situ*. With this method, we obtain clean and low-resistance contacts. From the analysis of conductance histograms and differential-conductance (dI/dV) traces, we deduce the preferred conductance value of a single C_{60} molecule between gold electrodes to be close to $0.1 G_0$. The presence of C_{60} is evidenced by features in the derivative of the dI/dV at energies close to the molecular vibration energies. The characteristics of the molecules disappear upon cold working of the junctions.

DOI: [10.1103/PhysRevB.76.125432](https://doi.org/10.1103/PhysRevB.76.125432)

PACS number(s): 73.63.-b, 73.23.-b, 74.70.Wz, 85.65.+h

Over the last years, much progress has been achieved in the understanding of the electronic transport through single molecules. Since the seminal experiment by Joachim *et al.*¹ in which a C_{60} molecule was contacted by a scanning-tunneling microscope tip, the fullerenes have become benchmark systems for the development of new measurement schemes for molecular electronics applications. Much theoretical work has been performed on different metal- C_{60} systems including the noble metals² and aluminum.³ It has been measured that C_{60} between gold electrodes would form ionic contacts, giving rise to high conductances.^{4,5} Due to its high symmetry, only a few different contact geometries have to be explored although the molecule bears manifold possible functionality including the possibility of endodoping by magnetic^{6,7} or other ions.⁸ Most of the single-molecule transport experiments performed so far can be categorized into two groups: The first set of experiments is characterized by rather high resistance contacts allowing for the investigation of Coulomb blockade (CB) and molecular level spectroscopy by inelastic electron tunneling spectroscopy. These devices can be fabricated by different techniques including scanning-tunneling microscopy (STM) and spectroscopy,¹ electromigrated electrode structures,^{9,10} and mechanically controllable break junctions (MCBJs).¹¹ Among those, STM provides the largest variability in the combination of metals and molecules, to tune the contact after its formation, to reestablish a new contact after it has been broken, and to image the configuration of the environment. With electromigrated electrodes, very stable devices are achieved but without any possibility to tune the coupling after the contact has been established and with usually very low yield. The MCBJ technique interpolates between these two extremes. It combines tunability of the contacts with high mechanical stability, enabling measurements over several hours on the same contact configuration at low temperatures and the application of external fields.

For the study of CB, oxide or other contamination layers between electrodes and molecules might be helpful for ensuring the weak coupling which is necessary for considering the molecular systems as independent from the metal electrodes. However, for the application of single-molecule contacts in electronic devices, the high dissipation which goes along with high-resistance contacts (even if the dissipation is distributed over a larger space including the electrodes) is an important restriction. Therefore, in the second set of experi-

ments, strong coupling, i.e., low-resistance contacts between the molecules and the metal electrodes, is required to explore the possibility of coherent transport through the whole device. Quantum-mechanically coherent transport would also give rise to manifold applications, e.g., by tuning the inherent properties of the molecules and thus constructing new functionality.¹²

Besides a suitable choice of the metal-molecule system, strong coupling between molecule and metal can only be achieved by fulfilling the following prerequisites. (1) Clean metal surface: This criterion can be fulfilled by working under ultrahigh vacuum (UHV) conditions with all three techniques mentioned above.¹³⁻¹⁵ (2) The contact area should not come in contact with liquid or gaseous solvents. The Leiden group uses direct deposition from the gas phase onto cold MCBJs for small molecules which are at room temperature in their gas phase. With this method, single-molecule hydrogen contacts with a conductance as high as one quantum of conductance $G_0=2e^2/h \approx 77.5 \mu\text{S}$ have been reported.¹⁴ However, larger molecules such as C_{60} are usually deposited from a liquid solution. The resulting contacts are therefore prone to contamination by residuals, ending up in general in high-resistance contacts.^{10,15} Only in a few occasions conductance values of the order of $0.1 G_0$ have been observed;¹⁵ here, the contact was opened by electromigration in a cryogenic vacuum. In a recent STM study, C_{60} molecules have been evaporated in UHV onto copper surfaces and high conductance values of the order of $0.25 G_0$ have been found.¹³

In our experiment, we evaporate the molecules *in situ* onto a cold MCBJ, resulting in very clean contacts. By comparison of conductance histograms and differential-conductance traces, we deduce that the conductance of a single C_{60} molecule between gold electrodes is close to $0.1 G_0$. The evidence of the presence of the molecules disappears completely upon mechanical treatment of the contacts.

The measurements are performed with a MCBJ device. The breaking mechanism is mounted on a continuous-flow cryostat and introduced into an UHV chamber with a homemade thermal evaporation source suitable for the evaporation of molecules such as C_{60} .

The electrode devices are fabricated following the standard process for lithographic MCBJs.¹⁶ As electrode material, we used a 100 nm thick gold layer on a steel substrate covered by an insulating polyimide layer. After electrically contacting the sample, it is mounted on the sample holder

and transferred into the vacuum chamber for evacuation. The cryostat arrives at base temperatures of ≈ 10 K. The pressure gauge located at room temperature reads a pressure of the order of 10^{-10} mbar; the pressure in the vicinity of the sample within the radiation shield is expected to be lower by at least an order of magnitude. Experiments with aluminum electrodes which are known to be rather susceptible to contamination reveal no indication of oxidation after several days.

For the measurements of the histograms and the recording of conductance vs distance curves in the tunneling regime, we used a source-measure unit which enables resistance measurements from the closed bridge (a few ohms) up to teraohms. The dI/dV 's were taken with a standard lock-in amplifier. The signals were preamplified by a variable gain preamplifier allowing the recording of dI/dV 's in a range of kilo-ohms to gigohms.

After the cooldown process, the electrodes are broken to form a tunnel contact. For characterizing the electrodes, conductance histograms and dI/dV 's in the tunnel regime as well as in the single- or few-atom regime are recorded. The histograms show a dominant peak at $1 G_0$ which represents the single-atom contact known from literature.¹¹ The absence of well-pronounced peaks at multiples of G_0 demonstrates the cleanliness of the electrodes.¹⁷ In the dI/dV 's, we observe contact-specific conductance fluctuations with a typical fluctuation period of the order of 10–50 mV, similar to the observations of Ludoph and van Ruitenbeek.¹⁸ They are produced by interference between different electronic paths which are backscattered at the atomic contact or the electrodes. Similar fluctuations are observed in the tunneling regime with $G \ll G_0$ as well. It is very difficult to stabilize contacts with $G \ll G_0$, while contacts with $G \approx G_0$ are found regularly, have a long lifetime, and sustain larger bias voltages although the transport currents are obviously higher. The relative amplitude as well as the typical period of the oscillations increase with decreasing G , revealing that for the low-conductance contacts shorter interference paths contribute. We mention these observations because the dI/dV 's of the Au- C_{60} -Au contacts reveal a similar behavior, making it necessary to perform a detailed and careful analysis (see below).

In order to use the samples as electrodes for contacting individual molecules, the ratio between the change of distance between the electrodes and the motion of the bending beam has to be determined. This is performed as usual by measuring the distance variation of the tunnel resistance.¹¹ We estimate the precision of the determination of the electrode distance to be about 30%.

The C_{60} molecules are evaporated from a tungsten boat with a rate smaller than 0.001 ML/s (ML denotes monolayer) (measured by a quartz sensor) onto the electrodes in the tunnel regime. From statistical analysis of several thousand contacts, we deduce the information that coverages of 0.1 ML are suitable to find contacts containing a single or a small number of molecules in the contacts (see below). During the evaporation, the electrodes are usually kept separated by about 1 nm, i.e., at a distance of the diameter of C_{60} , while a small voltage of ≈ 100 mV is applied. Similar results were obtained by evaporating the molecules without applied

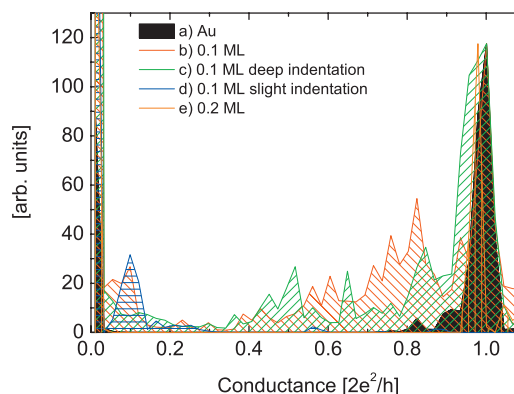


FIG. 1. (Color) Development of the histogram after several indentation and evaporation cycles of one sample. For deep indentation, the contacts are closed until the resistance reaches 200Ω , for slight indentation until $12 \text{ k}\Omega$. (a) Black, without C_{60} , (b) red, directly after evaporation, (c) green, after warming up and cooling down again, (d) blue, after application of high bias and using only few and careful indentation, and (e) orange, after additional evaporation. Between the evaporation steps, the break junction was opened and closed repeatedly. Through the opening and closing treatment, the prominent conductance peaks disappear nearly completely (for further details, see text).

voltage. However, the yield of contacts evidencing the presence of molecules in the junction is higher when using the protocol described first.

After evaporation, the electrode distance is reduced until a measurable conductance but with large fluctuations, both as a function of time and distance, is achieved ($1/G=R \approx 100 \text{ G}\Omega$). When the electrodes are closed further, the resistance drops down to a few hundred kilo-ohms and the fluctuations become markedly smaller. This change usually happens at a nominal electrode distance close to 0.5 nm and is taken as an indication for the formation of a molecular contact.¹⁹

For obtaining information about the conditions under which single-molecule contacts are formed, we study in detail the development of conductance histograms.

In Fig. 1, a selection of histograms recorded for one sample is plotted. We use opening curves (i.e., conductance traces measured when separating the electrodes from each other) as well as the same number of closing curves (i.e., recorded when approaching the electrodes toward each other) for constructing the histograms. After having collected data for pure gold contacts [histogram (a)], 0.1 ML C_{60} was evaporated. Briefly after the evaporation, conductance values below $1 G_0$ and a peak around $G=0.1 G_0$ in addition to the well-known maximum at $1 G_0$ [histogram (b)] appear. We interpret this peak at $0.1 G_0$ as the typical conductance of single-molecule contacts. The additional structure below $1 G_0$ presumably corresponds to disordered Au-Au contacts or multimolecule contacts.¹² It has been shown that mechanical treatment of clean atomic-size contacts of Au has the tendency to improve the crystallinity of the atomic contacts.¹¹ One would thus expect the $1 G_0$ peak to become stronger and narrower upon repeated closing and opening. However, the presence of the large fullerene molecules may hamper this

annealing mechanism. After closing the contact completely, warming up to room temperature, and cooling down again [histogram (c)], the peak at $0.1 G_0$ and the additional features below $1 G_0$ diminish and eventually disappear after several openings and closings. The peak at $0.1 G_0$ can be recovered upon applying a larger bias voltage. It remains present when the contact is closed only carefully to at most $0.9 G_0$ [histogram (d)]. When further continuing the mechanical treatment, all features below $1 G_0$ vanish. A possible explanation could be the formation of a molecular contact with rather high conductance as observed for the Pt- H_2 -Pt system.¹⁴ However, we observe that when the $0.1 G_0$ peak disappears in the histogram, all typical features in the dI/dV 's, which we attribute to the presence of molecules (see below), disappear as well. The combination of these two observations indicates that the molecules have been moved out of the contact area by the mechanical treatment. The observation of history-dependent histograms is important for the interpretation of histograms of contacts of larger molecules in general. For smaller and volatile molecules such as H_2 , this problem has not been reported, presumably because the molecules which have been removed from the contact by the cold-working procedure were replaced by new ones from the residual gas, or because the bond to the electrodes was strong enough to prevent the motion.¹⁴

When the molecules were driven out of the contact, it is possible to deposit new molecules on the same sample again *in situ*. Upon further evaporation in steps of 0.1 ML, it usually happens that the histograms show no structure below $1 G_0$ [histogram (e)] and also the dI/dV 's resemble those of pure gold contacts. A possible explanation would be that the larger fullerene coverage hinders the capture of a single molecule in the contact region. When using a C_{60} coverage as high as 0.5 ML, a rather constant background signal in the histogram between 0 and $1 G_0$ is found, and the maximum at $1 G_0$ vanishes as well (not shown), which we interpret in terms of larger than single molecule contacts and the impossibility of forming Au-Au contacts. Upon mechanical treatment, the details of the histogram, i.e., the relative height of individual peaks, are changed but the well-known histogram of pure Au is not restored anymore, indicating remaining molecules in the gap region. For this high coverage the dI/dV 's recorded shortly after the evaporation reveal large asymmetries (see the inset of Fig. 2) which may indicate an ionic bonding of C_{60} to the gold surface as has been deduced previously from STM measurements.^{4,5} In this situation, the C_{60} is better coupled to one of the electrodes and negatively charged due to electron transfer from the electrode. Depending on the sign of the applied voltage, further charge transfer can either be enhanced or suppressed, thus giving rise to asymmetric dI/dV 's. Calculations based on density-functional theory and assuming strong coupling of the fullerene to the metal electrodes reveal a density of states which is not symmetric with respect to the Fermi energy either.^{2,3} For particular energy dependence of the self-energies and by including charge transfer, this could give rise to asymmetric dI/dV 's as well.

Summarizing the results of the statistical analysis, we find that a coverage of 0.1 ML is a good choice for obtaining single-molecule contacts briefly after evaporation.

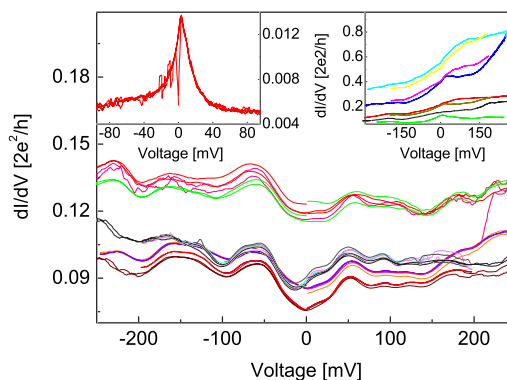


FIG. 2. (Color online) Differential-conductance traces for contacts formed after deposition of 0.1 ML C_{60} . The dI/dV has been measured with a lock-in amplifier. We used a modulation amplitude of 4 mV at $f=186$ Hz and integration times between 100 and 300 ms. The curves have been measured for 3 h when slowly closing the contact by 0.2 nm in total. Left inset: Example of a Kondo-like peak. Right inset: Examples of spectra measured for a coverage of 0.5 ML.

In the following, we therefore restrict ourselves to contacts formed after deposition of 0.1 ML and with only a few indentations of the electrodes. The differential conductance dI/dV reveals metallic behavior with a small modulation similar to the one observed for the metal electrodes without molecules (see Fig. 2). The depicted curves represent a subset of about 40 curves recorded subsequently for 3 h while slowly reducing the electrode distance.

The main differences to the behavior of the Au contacts are as follows. (1) High temporal stability of the contacts without drift. The overall conductance and parts of the fluctuation pattern only vary upon application of large bias voltages (≥ 300 mV) or by changing the electrode distance with the pushing rod. Without manipulating the electrodes, the curves remain constant for up to 30 min. (2) Higher stability with respect to the applied bias voltage. (3) Smaller contribution of variations on large voltage scale and smaller asymmetries. (4) Slightly smaller apparent voltage scale of the fluctuations. (5) Occasional observation of Kondo-like zero-bias anomalies similar to the observations in Ref. 15 (see the left inset of Fig. 2). In our experiment, the latter feature is very sensitive to small variations of the electrode distance. (6) Occasional observation of structures in the d^2I/dV^2 which we attribute to the excitation of vibration modes of the molecule (see below).

The majority of the structure in the dI/dV 's is most likely caused by electronic interference as mentioned before for the pure gold contacts. Contributions of long interference paths give rise to fluctuations on small energy scale and vice versa.¹⁸ In gold, the fluctuations at a typical voltage scale of $E_c=eV_c \approx 50$ meV arise from path lengths of the order of $L \approx \hbar v_F/E_c \approx 20$ nm (estimated for $v_F=1.4 \times 10^6$ m/s). While for the purely metallic contact the voltage drops in the vicinity of the constriction atoms, in the molecular contacts it partially takes place at the two metal-molecule interfaces, which are only about 1 nm apart. Thus, as long as the presence of the molecules does not markedly reduce the phase

coherence, no dramatic change in the fluctuation pattern can be assumed. This interpretation is supported by the observation that the overall conductance and the variations on larger voltage scales are more sensitive to changes of the geometry than the fluctuations at small voltage scale. The overall conductance is determined by the narrowest part of the contacts and can thus easily be varied by the rearrangements of individual atoms. For voltages higher than ≈ 150 mV, we observe time-dependent fluctuations showing up in Fig. 2 as an increased noise level. When reducing again the voltage, the fluctuations disappear without hysteresis. By applying voltages larger than 300–500 mV, the spectra change irreversibly, sometimes accompanied by an overall change of the conductance to a larger or smaller value. In a small fraction of experiments, the contact broke to a tunnel contact. After reducing the electrode distance, we recovered contacts with a conductance close to $0.1 G_0$ and revealing the typical features of the single- or few-molecule contacts. When opening or closing these contacts on a larger distance scale, the conductance remains rather constant for 1 or 2 Å, while for metal contacts in this conductance range, small variations of the distance led to a complete loss of the contacts.

Additional evidence for the presence of the molecules can be obtained when performing point-contact spectroscopy, e.g., by analyzing the second derivative of the current-voltage characteristics.^{12,14} When applying a bias voltage to a ballistic contact, the high-energy electrons may excite vibronic modes of the molecule forming the contact, giving rise to symmetric contributions to the nonlinear conductance at the energy of the vibration modes equally for both polarities of the voltage. Depending on the transmission, the effect can show up as a minimum¹⁴ or a maximum of the d^2I/dV^2 ,²² the transition between both being expected for a transmission close to 0.5.²³ In Fig. 3(a), we plot the numerical derivative of a subset of the dI/dV 's of Fig. 2. Minima and maxima of comparable size are observed at several voltage values, some of which slightly shift from curve to curve, while others appear independent of the exact contact configuration. Since the vibronic excitations are expected to give rise to symmetric features in the dI/dV with respect to bias reversal (antisymmetric in the d^2I/dV^2) we perform the following symmetry analysis: We calculate the numerical derivative of the symmetric and antisymmetric parts,

$$(dI/dV)_{s,a} = \frac{1}{2} \left[\frac{dI}{dV}(V) \pm \frac{dI}{dV}(-V) \right], \quad (1)$$

separately before we numerically derive $(d^2I/d^2V)_{s,a}$. A selection is shown in Fig. 3(b). In the symmetric part, two features at 34 and 114 mV are clearly observable, corresponding to energies of vibrational excitations of C_{60} .^{20,21} All other features, such as, e.g., the one at +64 mV in the non-symmetrized dI/dV , do not reveal a clear symmetry signature and must thus be of different origin. The peak at 34 mV corresponds to the lowest vibrational excitation, in which the molecule vibrates between a spherical and a prolate shape. This mode has recently been reported in Ref. 15, in which, at variance to our results, it showed up as a maximum in the differential conductance dI/dV . In Ref. 15, the vibrational

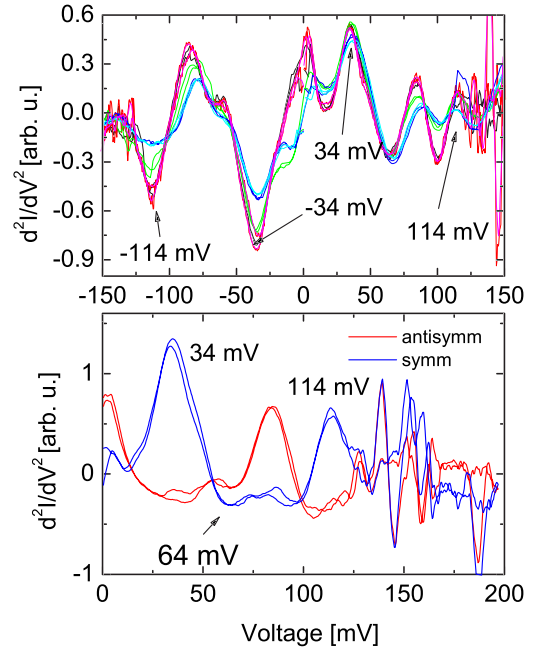


FIG. 3. (Color online) Upper graph: Derivatives of the dI/dV 's for a gold- C_{60} contact taken at a conductance of $0.1 G_0$. The curves have been measured consecutively for slight modifications of the electrode distance. Lower graph: Derivative of the symmetric and antisymmetric parts of one of the dI/dV 's of Fig. 2.

modes were observed in the same traces which also revealed a Kondo peak, thus, in a resonant transport condition. In a STM experiment, a structure at 54 meV was observed which was also interpreted as the excitation of a vibron mode.²² Two modes (at 113.3 meV and at 114.5 meV) lie in the energy range around 114 mV where we observe an additional symmetric structure. In a second set of curves measured on another contact, we observe the modes at 34 and 64 mV (not shown). Within the accuracy of our experiment, we do not observe a systematic shift of the symmetric structures upon deformation of the contact. Although in total 46 modes exist in the accessible energy range between 34 and 198 meV, we observe only a very small selection of them. Since we are not aware of any calculation of the electron-vibron coupling of C_{60} , we only can speculate that the other modes, which exist in the accessible voltage range, have a lower electron-vibron coupling constant. The fact that only a single, but different mode each has been observed in the two experiments reported in Refs. 15 and 22 indicates that the electron-vibron coupling constant might be very sensitive to the details of contact geometry.

In conclusion, we investigated the conductance of C_{60} molecules using a MCBJ technique with gold electrodes at 10 K in UHV. The C_{60} molecules were evaporated *in situ*. With this method, we obtain clean and highly conductive contacts without contamination. Conductance histograms and differential-conductance traces evidence that the conductance of a single C_{60} between Au electrodes is close to $0.1 G_0$, which is also proved by the observation of vibrational excitations of the molecule for contacts with this conductance value. The preferred conductance value is much larger

than reported in experiments, in which the electrodes had been exposed to atmosphere before the deposition of the molecules from solution.¹⁰ It is, however, in accordance with recent experiments performed with electromigrated break-junction electrodes¹⁵ and STM experiments.¹³ From theoretical considerations, metallic behavior with even higher linear conductance values of up to $2 G_0$ has been predicted when assuming particular highly symmetric contact geometries giving rise to perfect matching of the wave function and ionic bonding.² The authors predict that the high-conductance state is caused by the formation of a rather narrow resonance and would strongly depend on external gating. A single C₆₀ molecule contacted by clean noble-metal atoms can carry considerable currents of the order of microamperes. The analysis of the formation of conductance his-

tograms reveals that even at those low temperatures moving rather large molecules by cold working takes place, restricting statistical analysis to very limited ensembles. In order to further elucidate the transport mechanism, it would thus be helpful to perform noise measurements or other transport properties which reveal the counting statistics.

Note added in proof: During processing of this article the work by A. Galiardi *et al.*²⁴ and N. Sergueev *et al.*²⁵ appeared which addresses the question of which vibronic modes can be observed in electronic transport experiments.

Financial support by the Deutsche Forschungsgemeinschaft through SFB513 and the Krupp Foundation through the Alfred-Krupp-Förderpreis für Junge Hochschullehrer is gratefully acknowledged.

-
- ¹C. Joachim, J. K. Gimzewski, R. R. Schlittler, and C. Chavy, *Phys. Rev. Lett.* **74**, 2102 (1995).
- ²N. Sergueev, D. Roubtsov, and H. Guo, arXiv:cond-mat/0309614 (unpublished).
- ³J. Palacios, A. J. Pérez-Jiménez, E. Louis, and J. A. Vergés, *Nanotechnology* **12**, 160 (2001).
- ⁴E. I. Altman, and R. J. Colton, *Phys. Rev. B* **48**, 18244 (1993).
- ⁵A. J. Maxwell, P. A. Bruhwiler, D. Arvanitis, J. Hasselstrom, M. K.-J. Johansson, and N. Martensson, *Phys. Rev. B* **57**, 7312 (1998).
- ⁶D. S. Bethune, C. H. Kiang, M. S. de Vries, G. Gorman, R. Savoy, J. Vazquez, and R. Beyers, *Nature (London)* **363**, 605 (1993).
- ⁷T. Pradeep, G. U. Kulkarni, K. R. Kannan, T. N. Guru Row, and C. N. R. Rao, *J. Am. Chem. Soc.* **114**, 2272 (1992).
- ⁸R. F. Curl, *Carbon* **30**, 1149 (1992).
- ⁹H. B. Heersche, Z. de Groot, J. A. Folk, H. S. J. van der Zant, C. Romeike, M. R. Wegewijs, L. Zobbi, D. Barreca, E. Tondello, and A. Cornia, *Phys. Rev. Lett.* **96**, 206801 (2006).
- ¹⁰H. Park, J. Park, A. K. L. Lim, E. H. Anderson, A. P. Alivisatos, and P. L. McEuen, *Nature (London)* **407**, 57 (2000).
- ¹¹N. Agrait, A. Levy Yeyati, and J. M. van Ruitenbeek, *Phys. Rep.* **377**, 81 (2003).
- ¹²*Introducing Molecular Electronics*, edited by G. Cuniberti, G. Fagas, and K. Richter (Springer, Berlin, 2005).
- ¹³N. Néel, J. Kroger, L. Limot, T. Frederiksen, M. Brandbyge, and R. Berndt, *Phys. Rev. Lett.* **98**, 065502 (2007).
- ¹⁴R. H. M. Smit, Y. Noat, C. Untiedt, N. D. Lang, M. C. van Hemert, and J. M. van Ruitenbeek, *Nature (London)* **419**, 906 (2002).
- ¹⁵J. J. Parks, A. R. Champagne, G. R. Hutchison, S. Flores-Torres, H. D. Abruña, and D. C. Ralph, *Phys. Rev. Lett.* **99**, 026601 (2007).
- ¹⁶J. M. van Ruitenbeek, A. Alvarez, I. Piñeyro, C. Grahmann, P. Joyez, M. H. Devoret, D. Esteve, and C. Urbina, *Rev. Sci. Instrum.* **67**, 108 (1996).
- ¹⁷K. Hansen, S. K. Nielsen, M. Brandbyge, E. Laegsgaard, I. Stensgaard, and F. Besenbacher, *Appl. Phys. Lett.* **77**, 708 (2000).
- ¹⁸B. Ludoph and J. M. van Ruitenbeek, *Phys. Rev. B* **61**, 2273 (2000).
- ¹⁹J. Reichert, R. Ochs, D. Beckmann, H. B. Weber, M. Mayor, and H. v. Lohneysen, *Phys. Rev. Lett.* **88**, 176804 (2002).
- ²⁰Z. H. Dong, P. Zhou, J. M. Holden, P. C. Eklund, M. S. Dresselhaus, and G. Dresselhaus, *Phys. Rev. B* **48**, 2862 (1993).
- ²¹K.-A. Wang, A. M. Rao, P. C. Eklund, M. S. Dresselhaus, and G. Dresselhaus, *Phys. Rev. B* **48**, 11375 (1993).
- ²²J. I. Pascual, J. Gómez-Herrero, D. Sánchez-Portal, and H.-P. Rust, *J. Chem. Phys.* **117**, 9531 (2002).
- ²³L. de la Vega, A. Martín-Rodero, N. Agrait, and A. L. Yeyati, *Phys. Rev. B* **73**, 075428 (2006).
- ²⁴A. Gagliardi, G. C. Solomon, A. Pecchia, T. Frauenheim, A. Di Carlo, N. S. Hush, and J. R. Reimers, *Phys. Rev. B* **75**, 174306 (2007).
- ²⁵N. Sergueev, A. A. Demkov, and H. Guo, *Phys. Rev. B* **75**, 233418 (2007).